DOI 10.15622/ia.20.6.6

D. TRUNG, N. TUAN, N. BANG, T. TUYEN

SYNTHESIS OF LINE OF SIGHT ANGLE COORDINATE FILTER ON THE BASIS OF INTERACTIVE MULTI-MODEL EVALUATION ALGORITHM

Trung D., Tuan N., Bang N., Tuyen T. **Synthesis of Line of Sight Angle Coordinate Filter on the Basis of Interactive Multi-Model Evaluation Algorithm.**

Abstract. On the basis of the tracking multi-loop target angle coordinate system, the article has selected and proposed an interactive multi-model adaptive filter algorithm to improve the quality of the target phase coordinate filter. In which, the 3 models selected to design the line of sight angle coordinate filter; Constant velocity (CV) model, Singer model and constant acceleration model, characterizing 3 different levels of maneuverability of the target. As a result, the evaluation quality of the target phase coordinates is improved because the evaluation process has redistribution of the probabilities of each model to suit the actual maneuvering of the target. The structure of the filters is simple, the evaluation error is small and the maneuvering detection delay is significantly reduced. The results are verified through simulation, ensuring that in all cases the target is maneuvering with different intensity and frequency, the line of sight angle coordinate filter always accurately determines the target angle coordinates.

Keywords: flight equipment, target, maneuver, angle of line of sight, interactive multi-model.

1. Introduction. In the flight equipment, the target angular coordinate determination system is actually the tracking system that determines the target coordinate parameters. In an angle measuring device, the directional device generates signals that are proportional to the target tracking error according to the angle. This error in the vertical plane is determined by the angle $\Delta\varphi_d$, between the signal balance direction of the antenna and the target direction [1-3]. Figure 1, O_a and O_t - the position of the control object (flight equipment) and the target in the non-rotation coordinate system $X_0 O_a Y_0$, attached to the flight equipment.

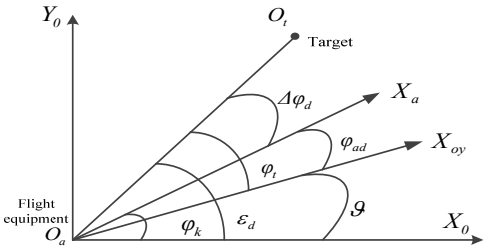

Fig. 1. Motion correlation between the flight equipment and the target

where: $O_a X_{oy}$ - longitudinal axis of the flight equipment;

$O_a X_a$ - the signal balance directional of the directional device;

ε_d - angle of the line of sight to target in the inertial coordinate system $X_0 O_a Y_0$;

φ_t - angle of the line of sight compared to the longitudinal axis of the flight equipment;

φ_{ad} - the angle of rotation of the antenna compared to the longitudinal axis of the flight equipment (the directional angle of the antenna);

ϑ - flight equipment nodding angle;

$O_a O_t$ - the flight equipment line of sight;

$\Delta\varphi_d$ - angle difference between the signal balance line and the line of sight.

The task of the problem determines the coordinates of the target angle: Generates angle ε_d and ω_d speed coordinate evaluations of the line of sight. On the current flight equipment control systems, the determination of ε_d and ω_d is done by the tracking one-loop angular coordinate determination system [4-7]. With this method, ε_d and ω_d are received using directly the signals from the antenna transmission system φ_{ad} and from gyros measure the longitudinal axis angle ϑ. The evaluation error ε_d and ω_d of this method will be large, especially in the case of the maneuvering target, due to the fact that the antenna has large inertia [3, 8-11].

Based on the application of optimal control theory and optimal filtration theory, the target angle coordinate determination system on current flight equipment is built with the tracking multi-loop [12, 13]. This coordinate determination system has a smaller error than the tracking one-loop system, especially in the case of a maneuvering target, because ε_d and ω_d are evaluated by a separate tracking loop without using directly the φ_{ad} signal as an evaluation signal [3, 14].

However, the tracking multi-loop coordinate determination system only takes into account the maneuvering target situation with specific values of maneuvering intensity ($\sigma_{j_t}^2$) and maneuvering frequency (α_j). That is, it remains unresolved for the class of the problem taking into account the diverse maneuverability in the reality of the target. Therefore, when the actual maneuvering of the target is not consistent with the hypothetical

model used to synthesize the coordinate system, the evaluation error ε_d and ω_d will increase.

Therefore, the task set out for the article: based on the tracking multi-loop coordinate determination system, building an algorithm to improve the accuracy of the target angle coordinates in maneuvering target conditions.

When applying optimal control theory and optimal filter theory, the problem of synthesizing systems to determine the target angle coordinates can be divided into two problems, namely:

The antenna control problem so that the signal balance line ($O_a X_a$) coincides with the direction of the line of sight ($O_a O_t$). This problem has been solved 3] or the optimal control technique [4, 9] can be used to synthesize the control law, so the article does not set out, but only applies the results when necessary.

The problem of evaluating the phase coordinate of the line of sight ε_d, ω_d takes into account the interaction of other parameters (ϑ, φ_{ad} ...) and the maneuvering of the target. This problem is solved by the article in the direction of synthesizing the adaptive system to improve the accuracy of the target angle coordinates in maneuvering target conditions.

The general method to improve the evaluation ε_d, ω_d in maneuverable target conditions is to use adaptive Kalman filtering techniques. Single-model adaptive filtering techniques perform the adaptation on the corrected phase or predictive of the Kalman filter algorithm [4, 15-18]. With these methods, the structure of the filter is relatively simple, however, the evaluation accuracy is not high and the maneuvering detection time is kept slow compared to the multi-model adaptive filtering techniques. In the multi-model adaptive filtration technique, with the assumption that the process follows one of the N known models, the evaluation accuracy is higher and the maneuvering detection delay is significantly reduced [3, 19-20].

2. Synthesis of the line of sight angle coordinate filter.

2.1. Selection of different models for the interactive multi-model evaluation algorithm. The purpose of the line of sight angle coordinate filter is to evaluate the line of sight angle, line of sight angle speed and target normalization acceleration in order to provide the information required for the flying equipment guide law. With the optimal target angular coordinate system, this filter is designed with the Singer model with fixed parameters. Then, the model's equation of state takes the form [3, 12]:

$$\dot{\varepsilon}_d = \omega_d \,, \tag{1}$$

$$\dot{\omega}_d = -\frac{2\dot{D}}{D}\omega_d + \frac{1}{D}(j_t - j_d) \,, \tag{2}$$

$$\dot{j}_t = -\alpha_j j_t + \xi_{j_t} \,, \tag{3}$$

where: D - relative distance between flight equipment and target;

j_t - normal acceleration of the target;

j_d - normal acceleration of the flight equipment; ξ_{j_t} - process noise of the model.

Based on this idea, the article adds 2 other models, characteristics for the small and large degree of maneuverability of the target. The model with constant velocity (CV model) and almost constant acceleration model (CA model) to build the interactive multi-model (IMM) evaluation algorithm for the line of sight angle coordinate filter. This choice is derived from the point of view, these 3 models are suitable for 3 different levels of maneuverability of the target.

Thus, the line of sight angle coordinate filter includes 3 linear Kalman filters running in parallel using 3 models, respectively, the CV model, Singer model and CA model. The final state evaluation is a combination of component filters with weighting on the exact probabilities of each model. As a result, the evaluation quality of the target phase coordinates is improved because the evaluation process has a redistribution of the probabilities of each model to suit the actual maneuverability of the target. The specific kinetics model to build these 3 filters is as follows:

– The Kalman 1 filter uses a CV model for synthesis (Fig. 2). This model considers the target normalized acceleration as white noise $j_t = \xi$ [5, 12]. In this case, the velocity and angle of the target orbital inclination (θ_t) are almost constant due to $\dot{\theta}_t = \frac{j_t}{V_t}$ (assuming the target velocity is constant). This model characterizes the degree of maneuverability of the smallest targets.

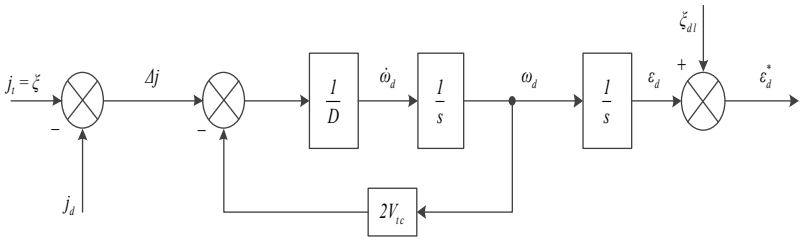

Fig. 2. CV model to synthesize the Kalman filter 1

The model's equation of state takes the form:

$$\dot{\varepsilon}_d = \omega_d \,, \tag{4}$$

$$\dot{\omega}_d = -\frac{2\dot{D}}{D}\omega_d - \frac{1}{D}j_d + \frac{1}{D}\xi = \frac{2V_{tc}}{D}\omega_d - \frac{1}{D}j_d + \frac{1}{D}\xi \,. \tag{5}$$

Where: $\frac{\xi}{D}$ - line of sight angular acceleration noise, due to the uncertainty in the model CV causes, $V_{tc} = -\dot{D}$ - target approach speed.

The vector form of the system of equations above:

$$\dot{\boldsymbol{x}}_1 = \boldsymbol{F}_{mh1}\boldsymbol{x}_1 + \boldsymbol{G}_{mh1}\boldsymbol{u}_1 + \boldsymbol{w}_1 \,. \tag{6}$$

Where: $\boldsymbol{x}_1 = \begin{bmatrix} \varepsilon_d \\ \omega_d \end{bmatrix}$ - target phase coordinate state vector;

$\boldsymbol{u}_1 = j_d$ - control signal;

$\boldsymbol{F}_{mh1} = \begin{bmatrix} 0 & 1 \\ 0 & \frac{2V_{tc}}{D} \end{bmatrix}$ - state transition matrix of filter 1;

$\boldsymbol{G}_{mh1} = \begin{bmatrix} 0 \\ -\frac{1}{D} \end{bmatrix}$ - control matrix;

$\boldsymbol{Q}_{mh1} = \begin{bmatrix} 0 & 0 \\ 0 & \frac{\sigma_{a_1}^2}{D^2} \end{bmatrix}$ - covariance matrix of process noise.

The discrete model above with cycle T, the base matrix is calculated as follows:

$$\boldsymbol{\Phi}_{mh}(t) = L^{-1}\left\{(p\boldsymbol{I} - \boldsymbol{F}_{mh})^{-1}\right\}.$$

Inside: L^{-1} - inverse Laplace transformations, $\boldsymbol{I}$ - the unit matrix has dimensions consistent with $\boldsymbol{F}_{mh}$.

Replace the sampling cycle T with the variable t of the base matrix to get the transition matrix $\boldsymbol{\Phi}^{k}_{mh} = \boldsymbol{\Phi}(T)$.

The discrete form control matrix, received by the formula:

$$\boldsymbol{G}^{k}_{mh} = \int_{0}^{T} \boldsymbol{\Phi}_{mh}(t).\boldsymbol{G}_{mh} dt .$$

The discrete form of the covariance matrix of the process noise:

$$\boldsymbol{Q}^{k}_{mh} = \int_{0}^{T} \boldsymbol{\Phi}_{mh}(t).\boldsymbol{Q}_{mh}.\boldsymbol{\Phi}^{T}_{mh}(t) dt .$$

According to the above general formulas, the parameters of the CV model discrete form:

$$\boldsymbol{\Phi}_{mh1} = \begin{bmatrix} 1 & \dfrac{D(\beta - 1)}{2V_{tc}} \\ 0 & \beta \end{bmatrix}$$ - state transition matrix;

$$\boldsymbol{G}_{mh1} = \begin{bmatrix} \dfrac{T}{2V_{tc}} - \dfrac{D(\beta - 1)}{4V_{tc}^2} \\ \dfrac{1 - \beta}{2V_{tc}} \end{bmatrix}$$ - control matrix.

The covariance matrix of the process noise discrete form as follows:

$$\boldsymbol{Q}_{mh_1}(1, 1) = \left(\frac{D(\beta^2 - 1)}{4V_{tc}} - \frac{D(\beta - 1)}{V_{tc}} + T \right) \sigma^2_{a_1},$$

$$\boldsymbol{Q}_{mh_1}(1,2) = \boldsymbol{Q}_{mh_1}(2,1) = \left(\frac{\beta^2 - 1}{8V_{tc}^2} - \frac{\beta - 1}{4V_{tc}^2} \right) \sigma_{a_1}^2 ,$$

$$\boldsymbol{Q}_{mh_1}(2,2) = \frac{\beta^2 - 1}{4V_{tc} D} \sigma_{a_1}^2 .$$

Inside: $\beta = e^{\frac{2V_{tc}T}{D}}$, T - discrete cycle.

$\sigma_{a_1}^2$ - process noise variance, which is characteristic of the maneuvering intensity.

– Filter Kalman 2 uses the Singer model (Fig. 3) to describe the target's movement [5, 12-13]. This model characterizes the moderate maneuverability of the target, shown through the selection of two fixed parameters, maneuvering frequency α_j and maneuvering intensity $\sigma_{a_1}^2$. The kinetics of model 2 has the following form:

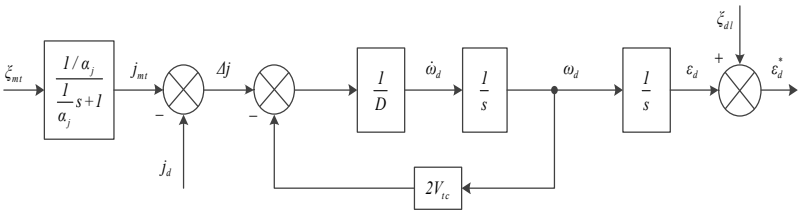

Fig. 3. Singer model to synthesize the Kalman filter 2

In the above model, the input inertia stage $(\frac{1/\alpha_j}{s/\alpha_j + 1})$ is the shaping filter. To create the target maneuvering style with constant intensity and the moment of maneuverability evenly distributed during flight time, the spectral density function of process noise ξ_{j_t} has the form:

$$\sigma_{a_2}^2 = \frac{j_{max2}^2}{T_f} .$$

Where: j_{max2} - maximized target normal acceleration, maneuverable; T_f - flight time.

Equation of state of model 2 (Singer model).
The above equation is in vector form:

$$\dot{\varepsilon}_d = \omega_d , \tag{7}$$

$$\dot{\omega}_d = \frac{2V_{tc}}{D}\omega_d + \frac{1}{D} j_t - \frac{1}{D} j_d , \tag{8}$$

$$\dot{j}_t = -\alpha_j j_t + \xi_{j_t} . \tag{9}$$

The above equation is in vector form:

$$\dot{\boldsymbol{x}}_2 = \boldsymbol{F}_{mh2}\boldsymbol{x}_2 + \boldsymbol{G}_{mh2}\boldsymbol{u}_2 + \boldsymbol{w}_2 .$$

Inside: $\boldsymbol{x}_2 = \begin{bmatrix} \varepsilon_d \\ \omega_d \\ j_{td} \end{bmatrix}$ - target phase coordinate state vector;

$\boldsymbol{F}_{mh_2} = \begin{bmatrix} 0 & 1 & 0 \\ 0 & \frac{2V_{tc}}{D} & \frac{1}{D} \\ 0 & 0 & -\alpha_j \end{bmatrix}$ - state transition matrix of filters 2;

$\boldsymbol{G}_{mh_2} = \begin{bmatrix} 0 \\ -\frac{1}{D} \\ 0 \end{bmatrix}$ - control matrix;

$\boldsymbol{Q}_{mh2} = \begin{bmatrix} 0 & 0 & 0 \\ 0 & 0 & 0 \\ 0 & 0 & 1 \end{bmatrix} \sigma_{a_2}^2$ - covariance matrix of process noise.

Similarly, we have the parameters of model 2 in discrete form:

$$\boldsymbol{\Phi}_{mh2} = \begin{bmatrix} 1 & \frac{D}{2V_{tc}}(\beta - 1) & \frac{e^{-\alpha T}}{\alpha(2V_{tc} + D\alpha)} - \frac{1}{2V_{tc}\alpha} + \frac{D\beta}{2V_{tc}(2V_{tc} + D\alpha)} \\ 0 & \beta & \frac{\beta - e^{-\alpha T}}{2V_{tc} + D\alpha} \\ 0 & 0 & e^{-\alpha T} \end{bmatrix},$$

$$\boldsymbol{G}_{mh2} = \begin{bmatrix} \frac{T}{2V_{tc}} + \frac{D(1-\beta)}{4V_{tc}^2} \\ \frac{1-\beta}{2V_{tc}} \\ 0 \end{bmatrix} \text{ - control matrix.}$$

Covariance matrix of the process noise discrete form as follows:

$$Q_{mh_2}(1,1) = \frac{(e^{-\alpha T} - 1)(\frac{8V_{tc}^2}{\alpha} + 4DV_{tc}) + T(D^2\alpha^2 + 4DV_{tc}\alpha + 4V_{tc}^2) - (\beta - 1)(\frac{D^3\alpha^2}{V_{tc}} + 2D^2\alpha)}{4D^2V_{tc}^2\alpha^4 + 16DV_{tc}^3\alpha^3 + 16V_{tc}^4\alpha^2}$$
$$- \frac{\frac{2V_{tc}^2}{\alpha}(e^{-2\alpha T} - 1) + \frac{D^3\alpha^2(\beta^2 - 1)}{4V_{tc}} + \frac{4D^2V_{tc}\alpha}{2V_{tc} - D\alpha}(e^{\frac{2V_{tc}T}{D} - \alpha T} - 1)}{4D^2V_{tc}^2\alpha^4 + 16DV_{tc}^3\alpha^3 + 16V_{tc}^4\alpha^2} \cdot \sigma_{a_2}^2,$$

$$Q_{mh_2}(1,2) = Q_{mh_2}(2,1) = \frac{D(e^{\frac{2V_{tc}T}{D} - \alpha T} - 1) - (\beta - 1)(\frac{D^2\alpha}{2V_{tc}} + D) - (e^{-\alpha T} - 1)(D + \frac{2V_{tc}}{\alpha})}{2D^2V_{tc}\alpha^3 + 8DV_{tc}^2\alpha^2 + 8V_{tc}^3\alpha}$$
$$+ \frac{\frac{V_{tc}(e^{-2\alpha T} - 1)}{\alpha} + \frac{D^2\alpha(\beta^2 - 1)}{4V_{tc}}}{2D^2V_{tc}\alpha^3 + 8DV_{tc}^2\alpha^2 + 8V_{tc}^3\alpha} \cdot \sigma_{a2}^2,$$

$$Q_{mh_2}(1,3) = Q_{mh_2}(3,1) = \frac{(e^{-\alpha T} - 1)(D + \frac{2V_{tc}}{\alpha}) - \frac{V_{tc}(e^{-2\alpha T} - 1)}{\alpha} + \frac{D^2\alpha(e^{\frac{2V_{tc}T}{D} - \alpha T} - 1)}{2V_{tc} - D\alpha}}{4V_{tc}^2\alpha + 2DV_{tc}\alpha^2} \cdot \sigma_{a2}^2,$$

$$Q_{mh_2}(2,2) = \frac{\frac{1 - e^{-2\alpha T}}{2\alpha} + \frac{D(\beta^2 - 1)}{4V_{tc}} - \frac{2D(e^{\frac{2V_{tc}T}{D} - \alpha T} - 1)}{2V_{tc} - D\alpha}}{D^2\alpha^2 + 4DV_{tc}\alpha + 4V_{tc}^2} \cdot \sigma_{a2}^2,$$

$$Q_{mh_2}(2,3) = Q_{mh_2}(3,2) = \left(\frac{e^{-2\alpha T} - 1}{2(D\alpha^2 + 2V_{tc}\alpha)} + \frac{D(\beta e^{-\alpha T} - 1)}{4V_{tc}^2 - D^2\alpha^2} \right) \sigma_{a_2}^2,$$

$$Q_{mh_2}(3,3) = \frac{1 - e^{-2\alpha T}}{2\alpha} \sigma_{a_2}^2.$$

– Filter 3 is synthesized based on the CA model (Fig.4). This model considers the target normal acceleration is almost constant (also known as the Jerk acceleration model is approximately equal to 0) [5, 12-13]. This model characterizes a high degree of maneuverability, when the target is to maneuver continuously at nearly constant acceleration.

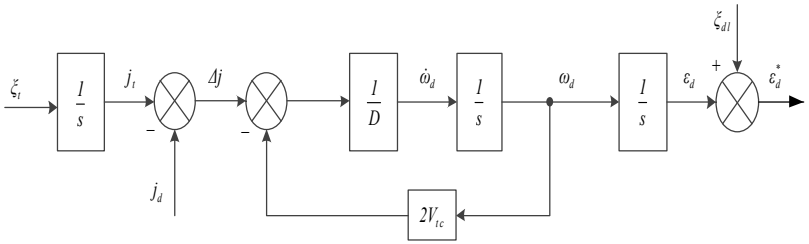

Fig. 4. CA model for synthesis of Kalman filter 3

Then, the model's equation of state takes the form similar to (7), (8):

$$\dot{\varepsilon}_d = \omega_d, \tag{10}$$

$$\dot{\omega}_d = \frac{2V_{tc}}{D}\omega_d + \frac{1}{D}j_t - \frac{1}{D}j_d, \tag{11}$$

$$\dot{j}_t = \xi_{j_t} . \quad (12)$$

In which, the input integral stage is the shaping filter. Similarly, to create the target maneuvering style with constant intensity and the moment of maneuverability evenly distributed during flight time, the spectral density function of process noise ξ_{j_t} has the form:

$$\sigma_{a_3}^2 = \frac{j_{max3}^2}{T_f} .$$

Where: j_{max3} - maximized target normal acceleration, maneuverable, T_f - flight time.

Note, when designing each filter, the spectral density of the process noise in the Singer and CA models is different, due to the different maneuvering intensity.

Equation of state in vector form:

$$\dot{\boldsymbol{x}}_3 = \boldsymbol{F}_{mh3}\boldsymbol{x}_3 + \boldsymbol{G}_{mh3}\boldsymbol{u}_3 + \boldsymbol{w}_3 . \quad (13)$$

Inside: $\boldsymbol{x}_3 = \begin{bmatrix} \varepsilon_d \\ \omega_d \\ j_{td} \end{bmatrix}$ - Target phase coordinate state vector.

$\boldsymbol{F}_{mh_3} = \begin{bmatrix} 0 & 1 & 0 \\ 0 & \frac{2V_{tc}}{D} & \frac{1}{D} \\ 0 & 0 & 0 \end{bmatrix}$ - State transition matrix of filters 3.

$\boldsymbol{G}_{mh3} = \begin{bmatrix} 0 \\ -\frac{1}{D} \\ 0 \end{bmatrix}$ - Control matrix.

$$\boldsymbol{Q}_{mh3} = \begin{bmatrix} 0 & 0 & 0 \\ 0 & 0 & 0 \\ 0 & 0 & 1 \end{bmatrix} \sigma_{a_3}^2$$ - Covariance matrix of process noise.

Switch to the discrete model, we have:

$$\boldsymbol{\Phi}_{mh3} = \begin{bmatrix} 1 & \frac{D(\beta - 1)}{2V_{tc}} & \frac{D(\beta - 1)}{4V_{tc}^{\,2}} - \frac{T}{2V_{tc}} \\ 0 & \beta & \frac{\beta - 1}{2V_{tc}} \\ 0 & 0 & 1 \end{bmatrix}$$ - State transition matrix.

$$\boldsymbol{G}_{mh3} = \begin{bmatrix} \frac{T}{2V_{tc}} + \frac{D}{4V_{tc}^2}(1 - \beta) \\ \frac{1 - \beta}{2V_{tc}} \\ 0 \end{bmatrix}$$ - Control matrix.

Covariance matrix of the process noise discrete form as follows:

$$Q_{mh_3}(1,1) = \left(\frac{D^3(\beta^2 - 1)}{64V_{tc}^5} + \frac{D^2T}{16V_{tc}^4} - \frac{D^2T\beta}{8V_{tc}^4} + \frac{DT^2}{8V_{tc}^3} + \frac{T^3}{12V_{tc}^2} \right) \sigma_{a_3}^2,$$

$$Q_{mh_3}(1,2) = Q_{mh_3}(2,1) = \left(\frac{D^2(\beta^2 - 1)}{32V_{tc}^4} + \frac{DT}{8V_{tc}^3} - \frac{DT\beta}{8V_{tc}^3} - \frac{D^2(\beta - 1)}{16V_{tc}^4} + \frac{T^2}{8V_{tc}^2} \right) \sigma_{a_3}^2,$$

$$Q_{mh_3}(1,3) = Q_{mh_3}(3,1) = \left(\frac{D^2(\beta - 1)}{8V_{tc}^3} - \frac{DT}{4V_{tc}^2} - \frac{T^2}{4V_{tc}} \right) \sigma_{a_3}^2,$$

$$Q_{mh_3}(2,2) = \left(\frac{D(\beta^2 - 1)}{16V_{tc}^3} - \frac{D(\beta - 1)}{4V_{tc}^3} + \frac{T}{4V_{tc}^2} \right) \sigma_{a_3}^2,$$

$$Q_{mh_3}(2,3) = Q_{mh_3}(3,2) = \left(\frac{D(\beta - 1)}{4V_{tc}^2} - \frac{T}{2V_{tc}} \right) \sigma_{a_3}^2 ,$$

$$Q_{mh_3}(3,3) = T\sigma_{a_3}^2 ,$$

where $\beta = e^{\frac{2V_{tc}T}{D}}$, T - discrete cycle.

2.2. The algorithm to evaluate the coordinates of the line of sight angle with 3 different models. On the basis of the interactive multi-model filtering algorithm [15, 19-21], we have a general block diagram describing the evaluation algorithm of the line of sight angle coordinates shown in Figure 5.

The process of implementing the evaluation algorithm of the line of sight angle speed filter is as follows:

Step 1. Call p_{ij} , ($i, j = 1,2,..., N$) – the probability of changing from the model i at time $(k - 1)$ to the model j at time k . This probability is constant throughout the evaluation process. We choose the model transfer probability matrix as follows:

$$\boldsymbol{\Pi} = \begin{bmatrix} 0,9995 & 0,0001 & 0,0004 \\ 0,0004 & 0,9995 & 0,0001 \\ 0,0001 & 0,0004 & 0,9995 \end{bmatrix}.$$

In which, model 1 is CV, model 2 is Singer and model 3 is CA.

Call $\mu_j(0)$ - model probability at the time of initialization. In the beginning, the true probabilities of the 3 models are equal, so:

$$\mu_{CV}(0) = \mu_{SINGER}(0) = \mu_{CA}(0) = \frac{1}{3}.$$

Step 2. Calculate the mixing probability, that is, the appearance probability of the i^{th} model at time $(k - 1)$ with the j^{th} model condition at time k .

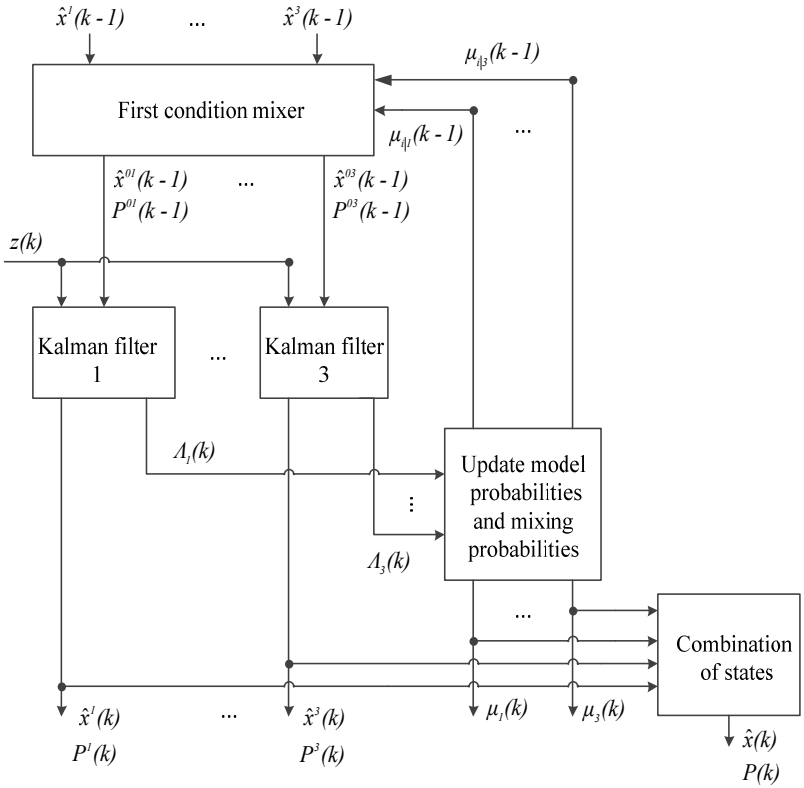

Fig. 5. Block diagram of line of sight angle coordinate filter with 3 component

Kalman filters: $\mu_{i|j}(k-1)$ is defined as:

$$\mu_{i|j}(k-1) = \frac{1}{\bar{c}_j} p_{ij}\mu_i(k-1); \; with \; i, j = 1,2,3; \tag{14}$$

$$\bar{c}_j = \sum_{i=1}^{3} p_{ij}\mu_i(k-1); \quad with \; j = 1,2,3.$$

Step 3. Mix the first condition for the j^{th} filter:

Input status, after mixing:

$$\hat{\boldsymbol{x}}^{0j}(k-1)=\sum_{i=1}^{3}\hat{\boldsymbol{x}}^{i}(k-1)\mu_{i|j}(k-1);\ With\ \ j=1,2,3\ ; \tag{15}$$

correlation of input errors, after mixing:

$$\hat{\boldsymbol{x}}^{0j}(k-1)=\sum_{i=1}^{3}\hat{\boldsymbol{x}}^{i}(k-1)\mu_{i|j}(k-1);\ With\ \ j=1,2,3\ ; \tag{16}$$

$$\begin{aligned}\boldsymbol{P}^{0j}(k-1)&=\sum_{i=1}^{3}\mu_{i|j}(k-1)\left\{\boldsymbol{P}^{i}(k-1)+\left[\hat{\boldsymbol{x}}^{i}(k-1)-\hat{\boldsymbol{x}}^{0j}(k-1)\right]\left[\hat{\boldsymbol{x}}^{i}(k-1)-\hat{\boldsymbol{x}}^{0j}(k-1)\right]^{T}\right\}\hat{\boldsymbol{x}}^{0j}(k-1)\\&=\sum_{i=1}^{3}\hat{\boldsymbol{x}}^{i}(k-1)\mu_{i|j}(k-1);\ With\ j=1,2,3.\end{aligned} \tag{17}$$

Due to the fact that the state vector size in the CV model is 2, and the Singer model and the CA model are 3, we need to solve the problem of mixing three models with different state vector sizes. In [15, 22-24] has proposed several ways to solve the problem. Here, we simply choose that when mixing for the CV model (model with smaller state space size), we only mix the corresponding state components in the Singer and CA model, ignoring the states remaining. When mixing for Singer and CA models (the model with larger state space size), we consider the missing state components in the CV model to zero.

Step 4. Perform evaluation algorithm of each component filter, with the first conditions, is mixed:

Evaluate the a priori of each filter:

$$\hat{\boldsymbol{x}}^{-j}(k)=\boldsymbol{\Phi}_{k}^{j}\hat{\boldsymbol{x}}^{j}(k-1)+\boldsymbol{G}_{k}^{j}\hat{\boldsymbol{u}}^{j}(k-1)\ ; \tag{18}$$

inside: $\boldsymbol{\Phi}_{k}^{j}$ - state transition matrix corresponding to the model j; $\boldsymbol{G}_{k}^{j}$ - control matrix corresponding to the model j.

Calculate the a priori error correlation matrix of each filter:

$$\boldsymbol{P}^{-j}(k)=\boldsymbol{\Phi}_{k}^{j}\boldsymbol{P}^{0j}(k-1)[\boldsymbol{\Phi}_{k}^{j}]^{T}+\boldsymbol{Q}_{k}^{j}(k-1)\ .$$

Calculate the Kalman amplification matrix:

$$\boldsymbol{K}^{j}(k)=\boldsymbol{P}^{-j}(k)\boldsymbol{H}_{j}^{T}(k)\times\left[\boldsymbol{H}_{j}(k)\boldsymbol{P}^{-j}(k)\boldsymbol{H}_{j}^{T}(k)+\boldsymbol{R}_{k}^{j}(k)\right]^{-1}. \tag{19}$$

Inside, $R_k^j(k) = \sigma_z^2$ - variance of observed channel noise. Here, we consider the variance of the measurement noise in all three models to be equal.

With the CV model, the Kalman amplification coefficient is only 2:

$$K_1^l(k) = \frac{P_{11}^{-l}(k)}{P_{11}^{-l}(k) + \sigma_z^2},$$

$$K_2^l(k) = \frac{P_{12}^{-l}(k)}{P_{11}^{-l}(k) + \sigma_z^2}.$$

The Singer and CA models are respectively:

$$K_1^j(k) = \frac{P_{11}^{-j}(k)}{P_{11}^{-j}(k) + \sigma_z^2},$$

$$K_2^j(k) = \frac{P_{12}^{-j}(k)}{P_{11}^{-j}(k) + \sigma_z^2},$$

$$K_3^j(k) = \frac{P_{13}^{-j}(k)}{P_{11}^{-j}(k) + \sigma_z^2}.$$

Evaluate the posterior state (after measurement update) of each filter:

$$\hat{\boldsymbol{x}}^j(k) = \hat{\boldsymbol{x}}^{-j}(k) + \boldsymbol{K}^j(k)\left[\boldsymbol{z}(k) - \boldsymbol{H}^j(k)\hat{\boldsymbol{x}}^{-j}(k)\right]. \quad (20)$$

The posterior correlation matrix of each filter:

$$\boldsymbol{P}^j(k) = \left[\boldsymbol{I} - \boldsymbol{K}^j(k)\boldsymbol{H}^j(k)\right]\boldsymbol{P}^{-j}(k).$$

Step 5. Calculate the logical function for the filter j^{th}:

$$\Lambda_j(k) = N\left[\boldsymbol{z}(k); \hat{\boldsymbol{z}}^j\left[k \mid k-1; \hat{\boldsymbol{x}}^{0j}(k-1 \mid k-1)\right], S^j\left[k, \boldsymbol{P}^{0j}(k-1 \mid k-1)\right]\right]. \quad (21)$$

It means, $\Lambda_j(k) = N\left[e^j(k); 0; S^j(k)\right]$, inside:

$$e_j(k) = z(k) - \boldsymbol{H}^j \hat{\boldsymbol{x}}^{-j}(k-1),$$

$$S_j(k) = \boldsymbol{H}_j \left[\boldsymbol{\Phi}_k^j \boldsymbol{P}^{0j}(k-1)[\boldsymbol{\Phi}_k^j]^T + \boldsymbol{Q}_k^j \right] \boldsymbol{H}_j^T + \boldsymbol{R}_k^j,$$

$$\Lambda_j(k) = \frac{1}{\sqrt{2\pi S_j(k)}} exp(-\frac{1}{2} e_j^T(k) S_j^{-1}(k) e_j(k)),$$

$$\Lambda_j(k) = \frac{1}{\sqrt{2\pi S_j(k)}} exp(-\frac{1}{2S_j(k)} e_j^2(k)).$$

Step 6. Updated j^{th} model probabilities:

$$\mu_j(k) = \frac{1}{c} \Lambda_j(k) \overline{c}_j; \tag{22}$$

$c = \sum_{j=1}^{3} \Lambda_j(k) \overline{c}_j$ - normalized constants.

Step 7. Combination of evaluation states and error correlation matrix after updating the correct probabilities of each model.

Combination of evaluation states:

$$\mu_j(k) = \frac{1}{c} \Lambda_j(k) \overline{c}_j. \tag{23}$$

Combination of error correlation:

$$\boldsymbol{P}(k) = \sum_{j=1}^{3} \mu_j(k) \left\{ \boldsymbol{P}^j(k) + \left[\hat{\boldsymbol{x}}^j(k) - \hat{\boldsymbol{x}}(k) \right] \left[\hat{\boldsymbol{x}}^j(k) - \hat{\boldsymbol{x}}(k) \right]^T \right\}.$$

3. Simulation results and analysis. To survey the quality of the tracking multi-loop target angle coordinate system using the interactive multi-model filtering algorithm, we will simulate the angular coordinate system with different maneuvering styles of the target in the horizontal plane (Fig. 6). Then, compare with the quality of the optimal angular

coordinate system (with fixed parameters based on Singer model) according to the criteria of mean square error (MSE).

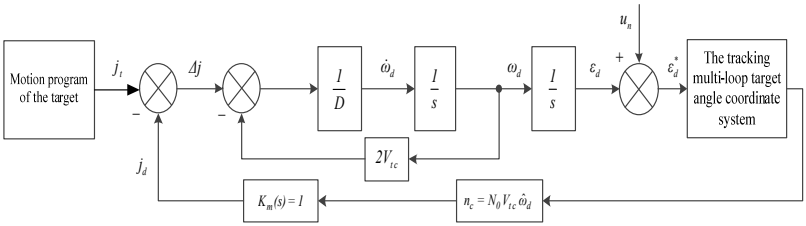

Fig. 6. Diagrams simulation of the target angle coordinates system in the ideal flight equipment control loop

3.1. In the case of a ladder type maneuvering target:

- The target's initial position: $x_t(0) = 40\ (km)$; $y_t(0) = 0\,(km)$.
- The flight equipment initial position: $x(0) = 0\,(km), y(0) = 0\,(km)$.
- The target flies in at velocity: $350\ (m/s)$.
- The flight equipment velocity: $1000\,(m/s)$.
- The target's initial trajectory tilt angle: $\theta_t = 0^o$.
- The normal acceleration of the target:

$$j_t = \begin{cases} 0 & when \quad t < 20\,s \\ 30\ (m/s^2) & when \quad t \geq 20\,s \end{cases}. \tag{24}$$

With this model, initially, the target has evenly straight movement. After 20 seconds, the target suddenly maneuvers continuously with constant normal acceleration $30\,(m/s^2)$. Thus, the target has a change from a non-maneuverable model to maneuverability with constant normal acceleration. This motion model has uncertainty in maneuvering moment and maneuvering intensity. The simulation results of the target angle coordinate system for the case of ladder-type maneuvering targets are as follows (Fig. 7, 8). Figures 10-17 reflect other features of the analyzed process.

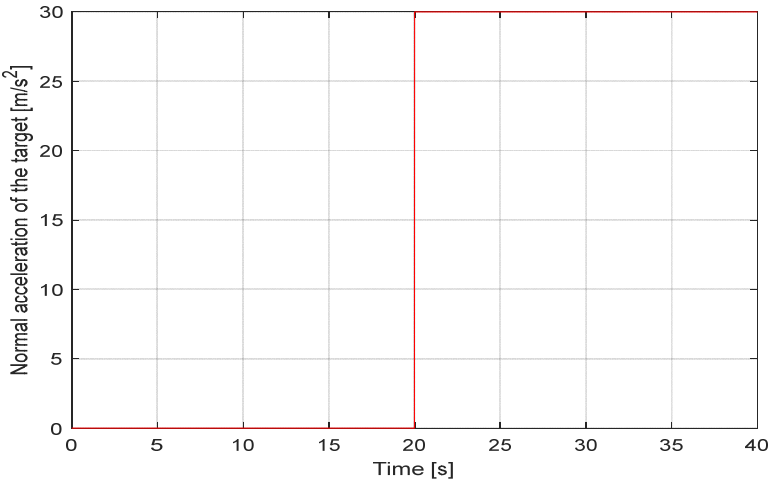

Fig. 7. Normal acceleration of the target

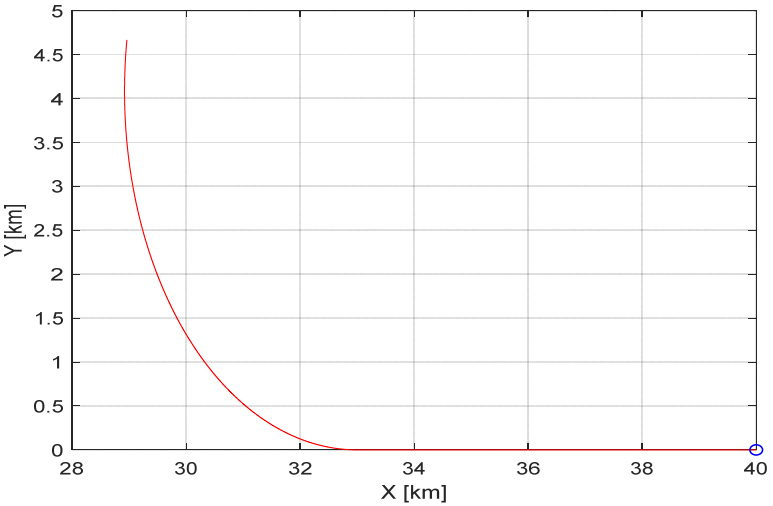

Fig. 8. Ladder-type maneuvering target trajectory

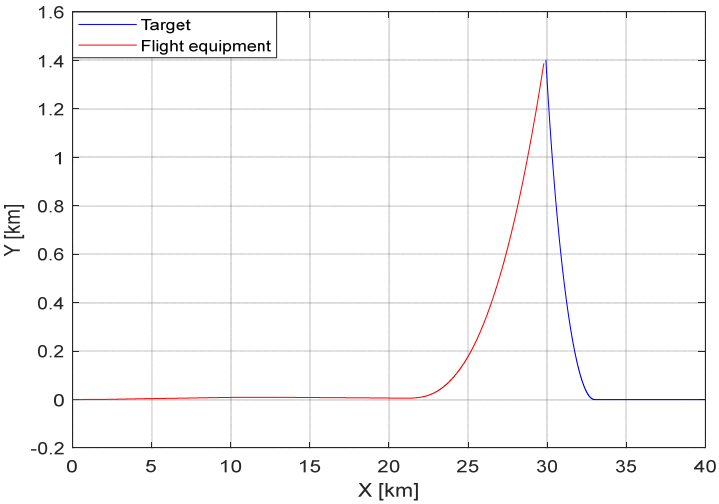

Fig. 9. Flight equipment - target trajectory

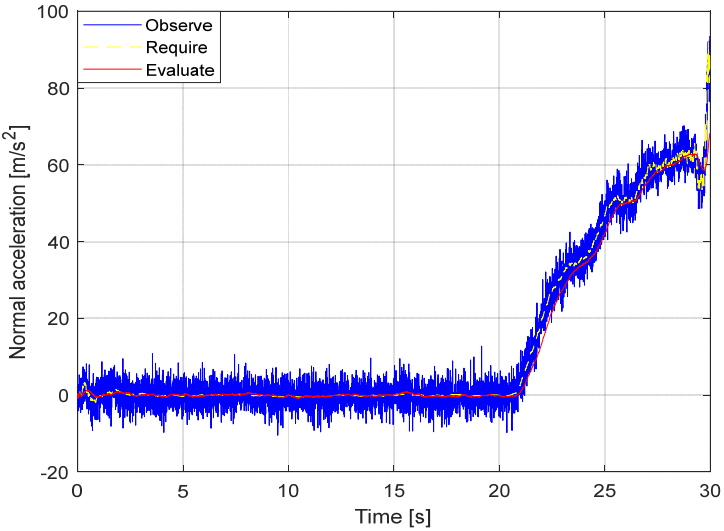

Fig. 10. Normal acceleration of the flight equipment

After 20 seconds of steady straight movement, the maneuvering target with constant normal acceleration. This causes the required normal acceleration of the small missile at an early stage (before 20 seconds), then increases continuously until the meeting point. However, the flight equipment normal acceleration filter still gives a good evaluation.

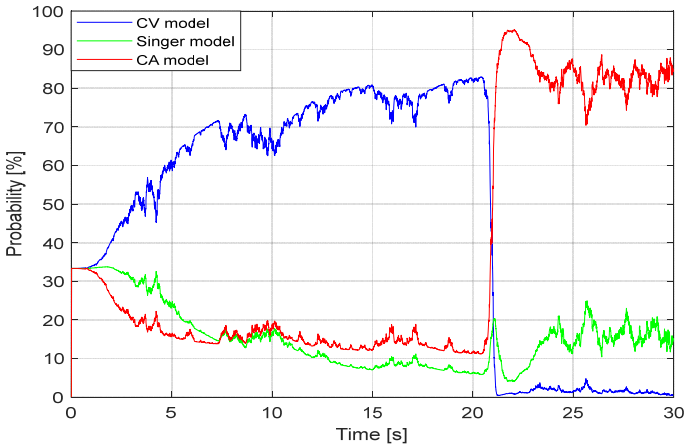

Fig. 11. The graph shows the correct probabilities of the model

Figure 11 shows that from 0 to 20 seconds, the CV model dominates, but after about 22 seconds (the transition time of the IMM algorithm is about 2 seconds), the probability of the CA model is clearly dominant compared to the other 2 models. This trend continues to maintain in the remaining maneuverable time of the target. This evaluation result of the algorithm reflects quite correctly with the actual maneuvering of the target.

The results of evaluating the target phase coordinate for the case of ladder-type maneuvering target are as follows:

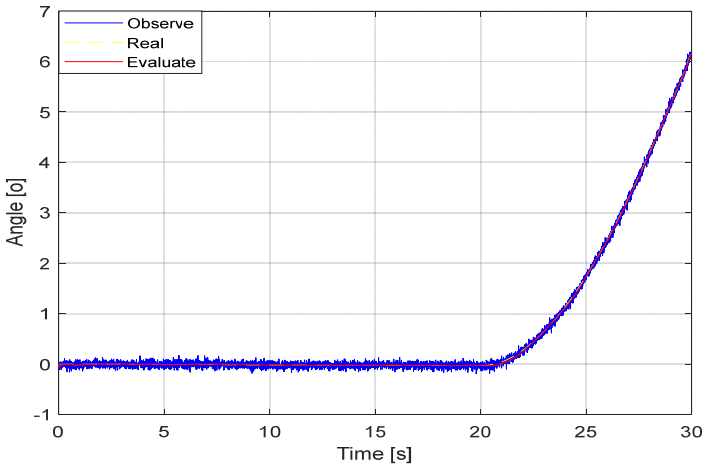

Fig. 12. Evaluate the angle of the line of sight

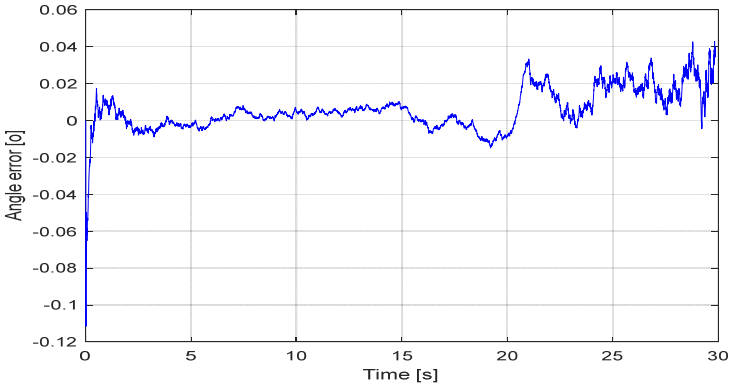

Fig. 13. Evaluation error of the line of sight angle

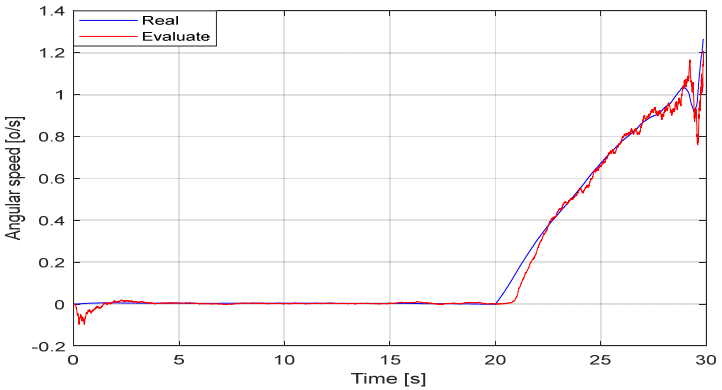

Fig. 14. Speed evaluation the angle of the line of sight

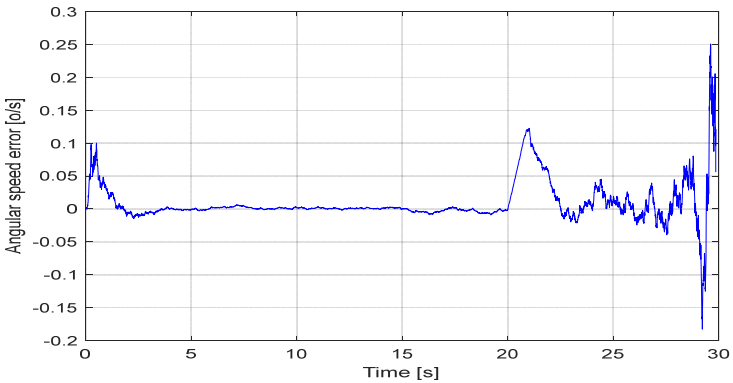

Fig. 15. Evaluation error of the line of sight angle speed

The simulation results show that in all 3 states: the angle of view, the angle of view and the normal acceleration of the target, the IMM evaluation algorithm gives a greater error at the time the target starts to maneuver (model change time). But right after that, the clinging error is smaller. Compare the quality of the IMM filter algorithm with the optimal filter algorithm after 100 Monte-Carlo runs:

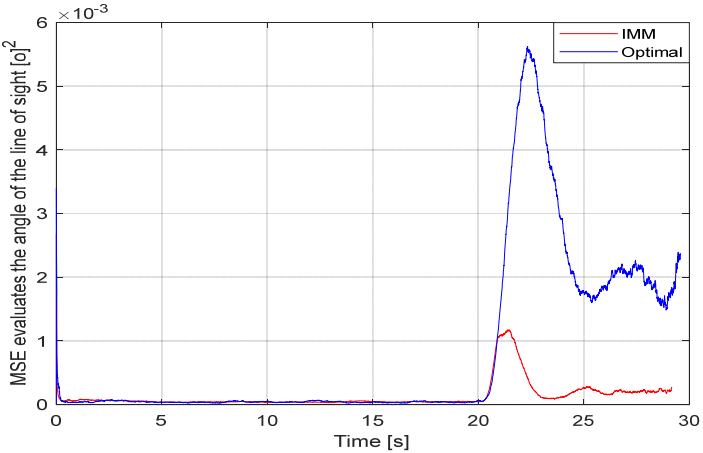

Fig. 16. Compare the MSE to evaluate the angle of the line of sight

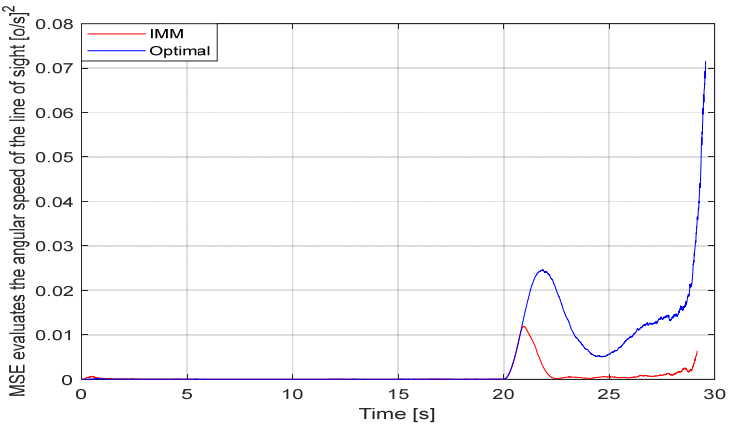

Fig. 17. Compare the MSE to evaluate the angular speed of the line of sight

Before the maneuvering target time (20s), the evaluation quality of the two algorithms was equivalent (the evaluation error of the optimal filtering algorithm was trivial smaller). But after 20 seconds, there is the

difference in evaluation quality. Detail:

– With the line of sight angle, the evaluation error of the IMM algorithm at the time of maneuvering model transfer (change) is $MSE(\varepsilon_d) \approx 1,2.10^{-3}[(o)^2]$, also the optimal filtering is $MSE(\varepsilon_d) \approx 2,5.10^{-3}[(o)^2]$. Then, at the stable tracking stage, the optimal filter algorithm for error is $MSE(\varepsilon_d) \approx 0,85.10^{-3}[(o)^2]$, the IMM algorithm is $MSE(\varepsilon_d) \approx 0,25.10^{-3}[(o)^2]$.

– With the angular speed of the line of sight, the evaluation error of the IMM algorithm at the time of maneuvering model transfer is $MSE(\omega_d) \approx 0,012\ [(o/s)^2]$, also the optimal filtering is $MSE(\omega_d) \approx 0,015\ [(o/s)^2]$. At the stable tracking stage, the optimal filter algorithm for error is $MSE(\omega_d) \approx 0,004\ [(o/s)^2]$, the IMM algorithm is $MSE(\omega_d) \approx 0,001\ [(o/s)^2]$.

– With the target normal acceleration, at the time of maneuvering model transfer, both algorithms give large evaluation errors $MSE(j_t) \approx 900\ [(m/s^2)^2]$. At the stable tracking stage, the optimal filter algorithm for error is $MSE(j_t) \approx 220\ [(m/s^2)^2]$, while the IMM filter gives a significantly smaller error with $MSE(j_t) \approx 10\ [(m/s^2)^2]$.

Obviously, when the maneuvering target with constant acceleration, the evaluation quality of the target angular coordinate system using the IMM filter algorithm improved when compared to the optimal filter algorithm.

3.2. In the case, the maneuvering target according to the Singer model. The parameters of the initial position, the velocity of the flight equipment and the target remain the same as before, but differ in the target normal acceleration.

The target normal acceleration is generated from the following kinematic model:

$$j_t(k) = (1 - T.\alpha_{j_t})j_t(k-1) + T \cdot u\ . \tag{25}$$

Where: $\alpha_{j_t} = 1\ (1/s)$, T - discrete integral cycle, u - control signal or maneuver command.

$$u = \begin{cases} 0 & when\ \ t < 5\,s \\ 40 \cdot \alpha_{j_t}\ (m/s^2) & when\ \ t < 15\,s \\ 0 & when\ \ t \geq 15\,s \end{cases}\ . \tag{26}$$

With this model, initially, the target has evenly straight movement. After 5 seconds, the target begins to maneuver in a Singer model with a command acceleration is $40(m/s^2)$. After 15 seconds, the target reverted to its non-maneuver style. Thus, this motion model has uncertainty in maneuvering moment, maneuvering time and maneuvering intensity.

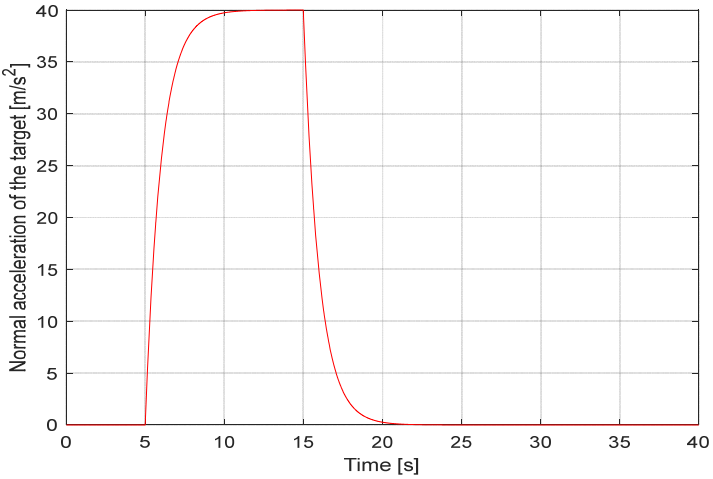

Fig. 18. Normal acceleration of the target

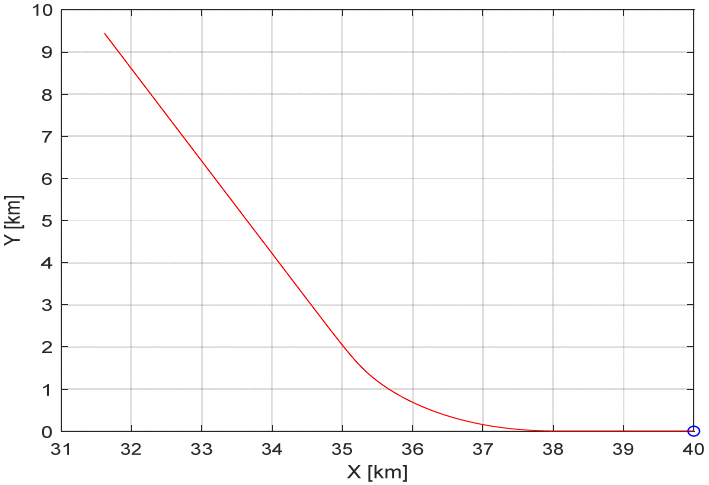

Fig. 19. Singer style maneuvering target trajectory

The simulation results of the target angle coordinate system for the maneuvering target case according to Singer model are as follows:

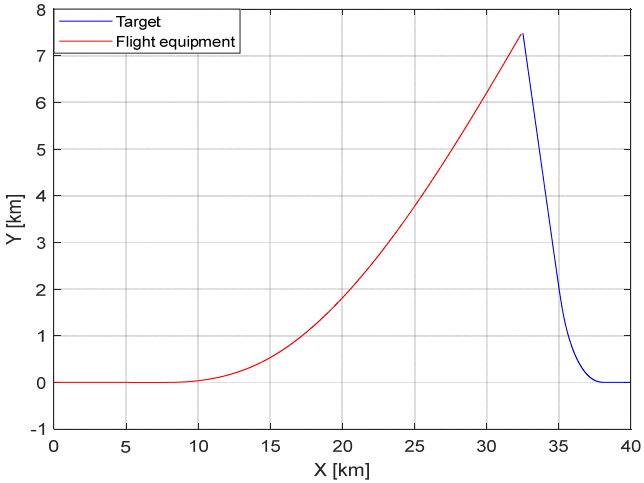

Fig. 20. Flight equipment - target trajectory

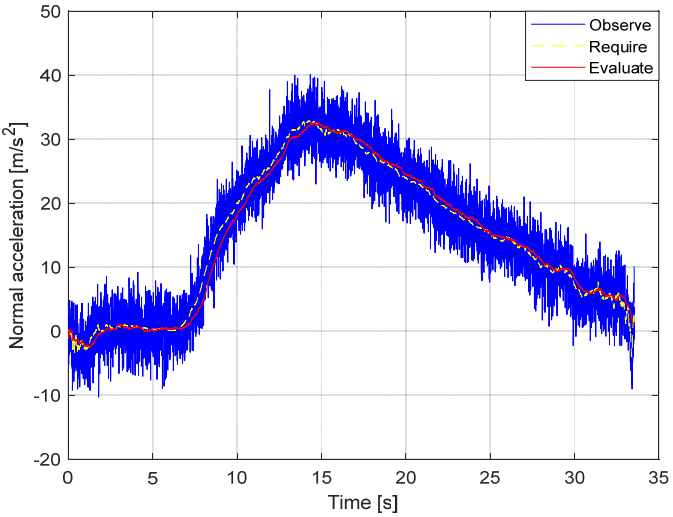

Fig. 21. Normal acceleration of the Flight equipment

When the target starts to maneuver, the normal acceleration requires an increase and when the target changes to the non-maneuver model, the required normalized acceleration of flight equipment tends to decrease to *0*.

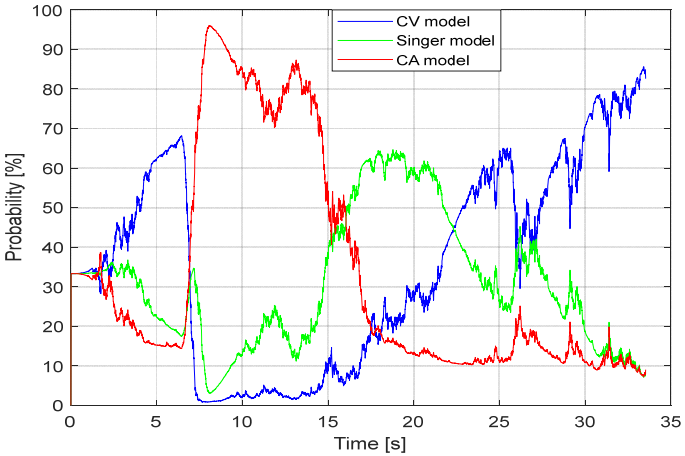

Fig. 22. Graphs update model probabilities

Obviously, when the target has evenly straight movement in the first 5 seconds, the CV model dominates over the other 2 models. In the time of the maneuvering target (5 ÷ 15s), the CA and Singer models dominate again, in which the weight of the CA model is greater because the target maneuvering command, in this case, is quite large ($40\,m/s^2$) makes the CA model fit with more practical. And when the target ends maneuver time, the correct probability belongs to the CV model.

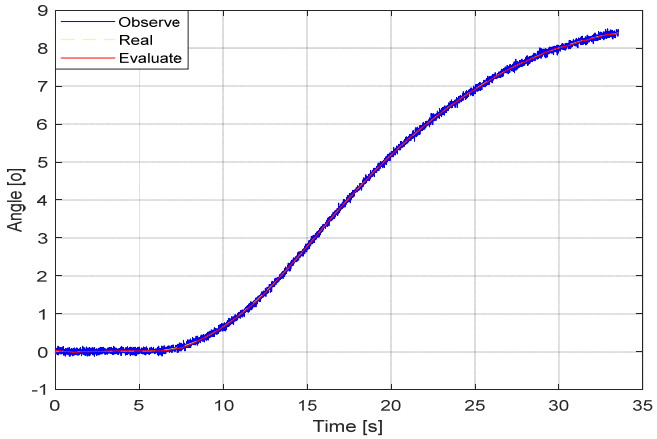

Fig. 23. Evaluate the angle of the line of sight

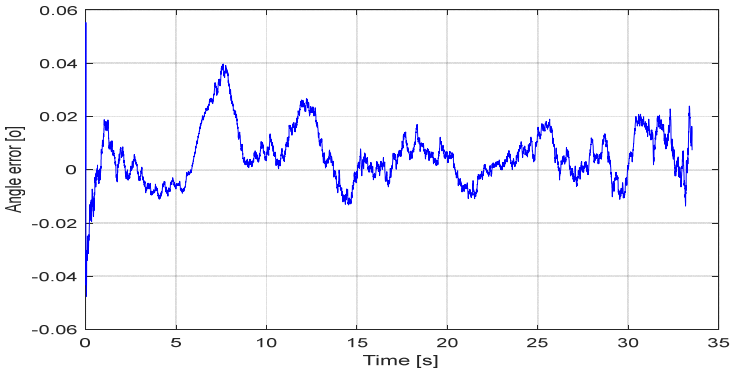

Fig. 24. Evaluation error the angle of the line of sight

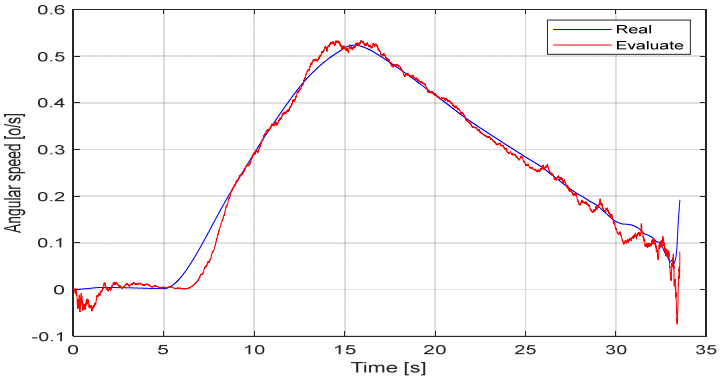

Fig. 25. Evaluate the angular speed of the line of sight

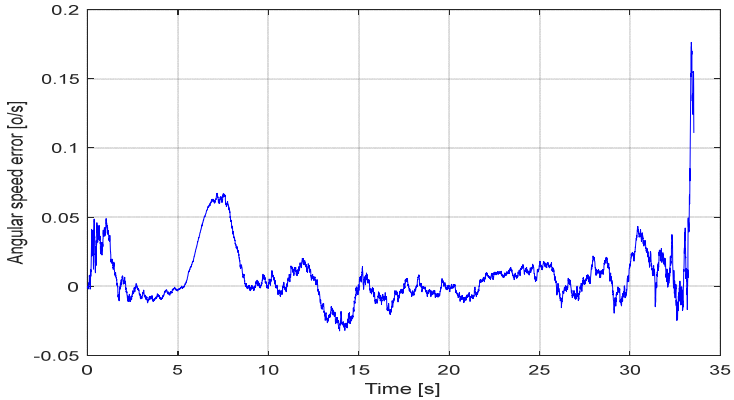

Fig. 26. Evaluation error the angular speed of the line of sight

Similar to the case of a maneuvering target with constant normal acceleration, in this case, all 3 target phase coordinates have a larger evaluation error at the time of model transfer (from non-maneuver to maneuver and on the contrary), but then IMM filter algorithm gives smaller evaluation error.

Comparing the quality of the IMM filter algorithm with the optimal filtration algorithm after 100 runs of Monte-Carlo for the case of Singer style maneuvering target gives the following results:

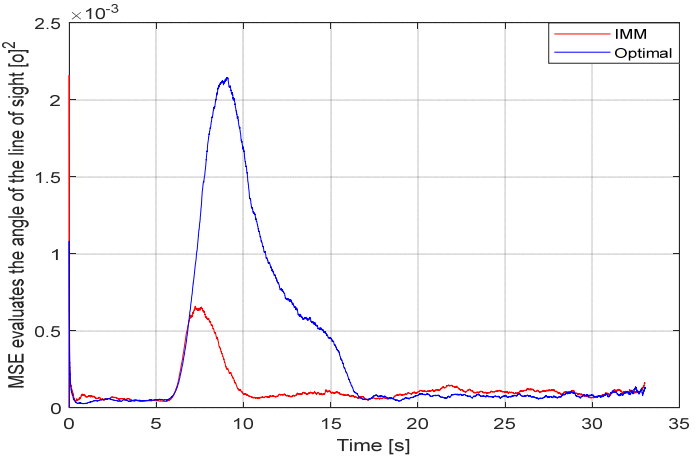

Fig. 27. Compare the MSE to evaluate the angle of the line of sight

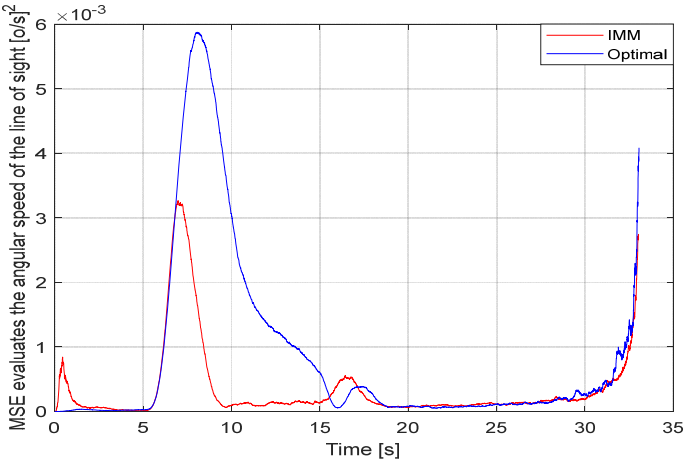

Fig. 28. Compare the MSE to evaluate the angular speed of the line of sight

MSE simulation results show that in the non-maneuver target stages (before 5 seconds and after 15 seconds), the evaluation quality of the line of sight angle coordinate filter when using the IMM filter algorithm is slightly worse when compared with the optimal filtering algorithm. However, at the maneuvering target stage (5 ÷15 seconds), the evaluation error of the IMM algorithm is significantly smaller. Detail:

– At the moment the target starts to maneuver, for the optimal filtering algorithm is $MSE(\varepsilon_d) \approx 2{,}2.10^{-3}\,(o)^2$, $MSE(\omega_d) \approx 6.10^{-3}\,(o/s)^2$, $MSE(j_t) \approx 1000\,(m/s^2)^2$; also for the IMM filtering algorithm is $MSE(\varepsilon_d) \approx 0{,}6.10^{-3}\,(o)^2$, $MSE(\omega_d) \approx 3{,}2.10^{-3}\,(o/s)^2$, $MSE(j_t) \approx 850\,(m/s^2)^2$.

– At the stable tracking stage, for the optimal filtering algorithm is $MSE(\varepsilon_d) \approx 0{,}7.10^{-3}\,(o)^2$, $MSE(\omega_d) \approx 1{,}7.10^{-3}\,(o/s)^2$, $MSE(j_t) \approx 600\,(m/s^2)^2$; also for the IMM filtering algorithm is $MSE(\varepsilon_d) \approx 0{,}1.10^{-3}\,(o)^2$, $MSE(\omega_d) \approx 0{,}15\times 10^{-3}\,(o/s)^2$, $MSE(j_t) \approx 30\,(m/s^2)^2$.

4. Conclusions. The article has synthesized the line of sight angle coordinates filter between the flight equipment and the target using the interactive multi-model adaptive filter technique. The suboptimal target angle coordinate tracking system is constructed from individual filters and combined with an antenna control system to create a multi-loop target angle coordinate system. Obviously, the target's maneuvering directly influences the evaluation filter the line of sight angle coordinate. So, in order to synthesize the target angle coordinate determination system with high accuracy in the maneuvering target conditions, just need to improve the line of sight angle coordinate evaluation filter, keeping the other filters.

The simulation results of the tracking multi-loop target angle coordinate system show that, when comparing the quality of the line of sight angle coordinate filter using the IMM filter algorithm based on the MSE criteria, the evaluation error is smaller than the optimal filtering algorithm under different maneuvering target conditions. Here, the change of the target maneuvering styles while the flight equipment approaches the target, highlighting the advantages and reliability of the interactive multi-model evaluation algorithm. The advantage is that during the evaluation process, the algorithm will always update the closest approximate model to the actual motion of the target, resulting in a combination of state evolution from the component filters giving results more precisely, the optimal filter has a fixed parameter. Of course, the more models that are taken into account when designing the line of sight angle coordinate filter, the higher the adaptability of the filter to target maneuverability, but we need to

consider the cost of calculation and real-time response of the electronic computer on board.

References

1. Liu T., Xie Y. A relative navigation algorithm for a chaser tracking a non-cooperative maneuvering target in space. 31(5). 2016. pp. 1338–1344.
2. Jiyuan L., Jun Z., Yingying L. Applying auto-adaptation filter to tracking of maneuvering target in special relative navigation. J. Northwest. Polytech. Univ. 4, 013. 2018.
3. Kanashekova A.I, Merkulov A.I. Aviatsionny'e sistemy radioupravleniya. [Airborne radio control systems]. Radio engineering. Moscow. 2013. (In Russ.).
4. Bar S.Y., RongLi X., Kirubarajan T. Estimation with Applications to Tracking and Navigation. Theory Algorithms and Software. John Wiley & Sons. 2011.
5. Blackman S., Popoli R. Design and analysis of modern tracking systems. Artech House. 2009.
6. Shaofeng M., Xinxi F., Yulei L., Zhang W., Xiaomei Z. A variable dimension adaptive IMM tracking algorithm. Electron. Opt. Control 22. (02). 2016. pp. 36-45.
7. Xiu L.H., Jing S.Y. Curve Model of Adaptive Interaction Model Algorithm Tracking Method. Applied Mechanics and Materials. Vol 738-739. March 2018. pp. 344-349.
8. Jiangw L.V.Z.., Lan Y. IMM-CKF algorithm based on variable dimension interaction. Comput. Appl. Softw. 30(5). 4–6. 2017.
9. Nguyen N.T., Nguyen D.T., Nguyen V.B. Synthesis of remote control law when taking into dynamics and nonlinearity of the missile stage. Intelligent Systems and Networks (ICISN 2021). Springer. March 2021. pp. 171-180.
10. Xiong, K., Wei, C. Spacecraft relative navigation based on multiple model adaptive estimator. J. Syst. Sci. Math. Sci. 34(07). 2018. pp. 828–837.
11. Sambasiva R., Raj K. Implementation of Adaptive Filter Algorithm for Underwater Acoustic System. International Journal of Recent Trends in Engineering. Vol 2. No.2. 2019. pp. 13-22.
12. Le X.R., Kilkov V.P. A survey of maneuvering target tracking: Approximation techniques for nonlinear filtering. Proceedings of SPIE conference on signal and data processing of small targets. 2014. pp. 537-550.
13. Li X.R., Jilkov V.P. Survey of maneuvering target tracking-part V. IEEE transaction on aerospace and electronic systems. 41 (4). 2015. pp. 1255-1321.
14. Xu B. An adaptive tracking algorithm for bearings-only maneuvering target. International journal of computer science and network security. 7 (1). 2017.
15. Yang C., Blasch E. Characteristic errors of the IMM algorithm under three maneuver models for an accelerating target. In: International Conference on Information Fusion. IEEE. 2018.
16. Yang C.C., Tsung T.K. An interactive dynamic multi-objective programming model to support better land use planning, Land Use Policy, Elsevier, Vol.36. 2016. pp. 13-22
17. Qian G.H., Li, Y., Luo, R.J. One maneuvering frequency and the variance adaptive filtering algorithm for maneuvering target tracking. J. Radars 2(6).2017. pp. 258–264.
18. Kim H.S., Chun Seung Yong. Design of fuzzy IMM algorithm based on Basic Sub-models and Time-varying mode transition probabilities. International journal of control automation and systems. 4 (5). 2016. pp. 559-566.
19. Lee J.B., Joo Y.H., Park J.B. IMM method using intelligent input estimation for maneuvering target tracking, ICCAS 2013. pp. 1278-1282.

20. Nguyen V.B., Nguyen T.T., Dang T.T. Synthesis of parameter recognition algorithm and state evaluation for flight device. East European Scientific Journal. Vol 2. No.66. 2021. pp. 10-17.
21. Nguyen V.B., Dang C.V. Synthesis of the maneuver target acceleration determines algorithm. Journal of natural and technical sciences. Sputnik Publishing House. No.2 (153). 2021. pp. 145-156.
22. Wu N.E., Youmin Z., Kermin Z. Detection, estimation and accommodation of loss of control effectiveness. International journal of adaptive control and signal processing. 14. 2010. pp. 775-795.
23. Kim, H.S., Park, J.G., Lee, D. Adaptive fuzzy IMM algorithm for uncertain target tracking. Int. J. Control Autom. Syst. 7(6). 2017. pp. 1001–1008.
24. Jiadong R., Xiaotong Z. Interactive multi-model target Maneuver tracking method based on the adaptive probability correction, International Conference on Swarm Intelligence, ICSI 2018. pp. 235-245.

Trung Dang — Ph.D., Lecturer, Electric Power University. Research interests: wind power, HVDC systems, power quality, application of modern optimal control in power systems. The number of publications — 4. dangtientrung@gmail.com; 235, Hoang Quoc Viet, 112400, Hanoi, Viet Nam; office phone: +8(491)566-8855.

Tuan Nguyen — Ph.D., Lecturer, Le Quy Don University of Science and Technology. Research interests: управление энергосистемой и анализ стабильности энергосистемы, реагирование на потребности интеллектуальной сети, система автоматизации зданий, возобновляемая энергия. The number of publications — 7. ngoctuanhvhn@gmail.com; 236, Hoang Quoc Viet, 112400, Hanoi, Viet Nam; office phone: +8(496)250-5955.

Bang Nguyen — Ph.D., Lecturer, Vietnam Air and Air Defense Forces Academy. Research interests: flying equipment control, intelligent control, signal processing, modeling and simulation. The number of publications — 19. banghvpkkq@gmail.com; 104, Nguyen Van Troi, 112400, Ho Chi Minh City, Viet Nam; office phone: +8(498)466-9384.

Tuyen Tran — Ph.D., Lecturer, Le Quy Don University of Science and Technology. Research interests: power system control and power system stability analysis, smart grid demand response, building automation system, renewable energy. The number of publications — 5. thaisonmos@gmail.com; 236, Hoang Quoc Viet, 112400, Hanoi, Viet Nam; office phone: +8(497)558-0368.

УДК 006.72 **DOI** 10.15622/ia.20.6.6

Д.Т. Чунг, Н.Н. Туан, Н.В. Банг, Т.В. Туйен

СИНТЕЗ ФИЛЬТРА КООРДИНАТ УГЛА ПРЯМОЙ ВИДИМОСТИ НА ОСНОВЕ ИНТЕРАКТИВНОГО МНОГОМОДЕЛЬНОГО АЛГОРИТМА ОЦЕНКИ

Чунг Д.Т., Туан Н.Н., Банг Н.В., Туйен Т.В. **Синтез фильтра координат угла прямой видимости на основе интерактивного многомодельного алгоритма оценки.**

Аннотация. На основе отслеживающей многоконтурной системы координат целевого угла в статье был выбран и предложен интерактивный многомодельный алгоритм адаптивного фильтра для улучшения качества фильтра целевых фазовых координат. Алгоритм интерактивной многомодельной оценки способен адаптироваться к динамике цели по мере продвижения процесса оценки к наиболее подходящей модели. Данный алгоритм имеет 3 модели, выбранные для разработки фильтра координат угла прямой видимости: модель постоянной скорости (CV), модель Зингера и модель постоянного ускорения, характеризующие 3 различных уровня маневренности цели. В результате, качество оценки фазовых координат цели улучшается, поскольку процесс оценки имеет перераспределение вероятностей каждой модели в соответствии с фактическим маневрированием цели. Структура фильтров проста, ошибка оценки мала, а задержка обнаружения маневрирования значительно сокращается. Результаты проверяются посредством моделирования, гарантируя, что во всех случаях цель маневрирует с разной интенсивностью и частотой, фильтр координат угла прямой видимости всегда точно определяет угловые координаты цели. Метод синтеза системы координат цели, использованный в статье, может быть расширен и применен к системам сопровождения целей в РЛС управления огнем, размещенных под землей.

Ключевые слова: летное оборудование, цель, маневр, угол прямой видимости, интерактивная мультимодель.

Чунг Данг Тянь — канд. техн. наук, преподаватель, Электроэнергетический университет. Область научных интересов: ветроэнергетика, системы постоянного тока, качество электроэнергии, применение современного оптимального управления в энергосистемах. Число научных публикаций — 4. dangtientrung@gmail.com; Хоанг Куок Вьет, 235, 112400, Ханой, Вьетнам; р.т.: +8(491)566-8855.

Туан Нгуен Нгок — канд. техн. наук, преподаватель, Вьетнамский государственный технический университет имени Ле Куй Дона. Область научных интересов: power system control and power system stability analysis, smart grid demand response, building automation system, renewable energy. Число научных публикаций — 7. ngoctuanhvhn@gmail.com; Хоанг Куок Вьет, 236, 112400, Ханой, Вьетнам; р.т.: +8(496)250-5955.

Банг Нгуен Ван — канд. техн. наук, преподаватель, Академия ВВС и ПВО. Область научных интересов: управление летательной аппаратурой, интеллектуальное управление, обработка сигналов, моделирование и симуляция. Число научных публикаций — 19. banghvpkkq@gmail.com; Нгуен Ван Трой, 104, 112400, Хошимин, Вьетнам; р.т.: +8(498)466-9384.

Туйен Тран Ван — канд. техн. наук, преподаватель, Вьетнамский государственный технический университет имени Ле Куй Дона. Область научных интересов: управление энергосистемой и анализ стабильности энергосистемы, реагирование на потребности

интеллектуальной сети, система автоматизации зданий, возобновляемые источники энергии. Число научных публикаций — 5. thaisonmos@gmail.com; Хоанг Куок Вьет, 236, 112400, Ханой, Вьетнам; р.т.: +8(497)558-0368.

Литература

1. Liu T., Xie Y. A relative navigation algorithm for a chaser tracking a non-cooperative maneuvering target in space // 31(5). 2016. pp. 1338–1344
2. Jiyuan L., Jun Z., Yingying L. Applying auto-adaptation filter to tracking of maneuvering target in special relative navigation // J. Northwest. Polytech. Univ. 4, 013. 2018.
3. Канащенкова А.И., Меркулова В.И. Авиационные системы радиоуправления // Радиотехника. Москва. 2013.
4. Bar S.Y., Rong L.X., Kirubarajan T. Estimation with applications to tracking and navigation // Theory Algorithms and Software. John Wiley & Sons. 2011.
5. Blackman S., Popoli R. Design and analysis of modern tracking systems // Artech House. 2009.
6. Shaofeng M., Xinxi F., Yulei L., Zhang W., Xiaomei Z. A variable dimension adaptive IMM tracking algorithm // Electron. Opt. Control 22.(02). 2016. pp. 36-45.
7. Xiu L. H., Jing S.Y. Curve model of adaptive interaction model algorithm tracking method // Applied Mechanics and Materials. Vol 738-739. March 2018. pp. 344-349.
8. Jiangw L.V.Z., Lan Y. IMM-CKF algorithm based on variable dimension interaction // Comput. Appl. Softw. 30(5). 4–6. 2017.
9. Nguyen. N.T., Nguyen D.T., Nguyen V.B. Synthesis of remote control law when taking into dynamics and nonlinearity of the missile stage // The International Conference on Intelligent Systems & Networks. Springer. March 2021.
10. Xiong K., Wei C. Spacecraft relative navigation based on multiple model adaptive estimator // J. Syst. Sci. Math. Sci. 34(07). 2018. pp. 828–837.
11. Sambasiva R., Raj K. Implementation of adaptive filter algorithm for underwater acoustic System // International Journal of Recent Trends in Engineering. Vol 2. No.2. 2019. pp. 13-22.
12. Le X.R., Kilkov V.P. A survey of maneuvering target tracking: Approximation techniques for nonlinear filtering // Proceedings of SPIE conference on signal and data processing of small targets. 2014. pp. 537-550.
13. Li X.R., Jilkov V.P. Survey of maneuvering target tracking-part V // IEEE transaction on aerospace and electronic systems. 41 (4). 2015. pp. 1255-1321.
14. Benlian X. An adaptive tracking algorithm for bearings-only maneuvering target // International journal of computer science and network security. 7 (1). 2017.
15. Yang C., Blasch E. Characteristic errors of the IMM algorithm under three maneuver models for an accelerating target // In: International Conference on Information Fusion. IEEE. 2018.
16. Yang C.C., Tsung T.K. An interactive dynamic multi-objective programming model to support better land use planning // Land Use Policy, Elsevier, Vol.36. 2016. pp. 13-22
17. Qian G.H., Li Y., Luo R.J. One maneuvering frequency and the variance adaptive filtering algorithm for maneuvering target tracking // J. Radars 2(6).2017. pp. 258–264.
18. Sik K.H., Yong C. S. Design of fuzzy IMM algorithm based on Basic Sub-models and Time-varying mode transition probabilities // International journal of control automation and systems. 4 (5). 2016. pp. 559-566.
19. Bum L. J., Hoon J. Y., Bea P. J. IMM method using intelligent input estimation for maneuvering target tracking // ICCAS 2013. pp. 1278-1282.

20. Nguyen V.B., Nguyen N. T. Synthesis of parameter recognition algorithm and state evaluation for flight device // East European Scientific Journal. Vol 2. No.66. 2021. pp. 10-17.
21. Nguyen V.B, Dang C.V. Synthesis of the maneuver target acceleration determines algorithm // Journal of natural and technical sciences. Sputnik Publishing House. No.2 (153). 2021. pp. 145-156.
22. Wu N.E., Zhang Y., Zhou K. Detection, estimation and accommodation of loss of control effectiveness // International journal of adaptive control and signal processing. 14. 2010. pp. 775-795.
23. Kim H.S., Park J.G., Lee D. Adaptive fuzzy IMM algorithm for uncertain target tracking // Int. J. Control Autom. Syst. 7(6). 2017. pp. 1001–1008.
24. Ren J., Zhang X. Interactive multi-model target maneuver tracking method based on the adaptive probability correction // International Conference on Swarm Intelligence, ICSI 2018. pp. 235-245.